Journal of ELECTRONIC MATERIALS, Vol. 47, No. 6, 2018
https://doi.org/10.1007/s11664-017-5929-3

TOPICAL COLLECTION: INTERNATIONAL CONFERENCE ON THERMOELECTRICS 2017

High-Temperature Formation Phases and Crystal Structure of Hot-Pressed Thermoelectric $CuGaTe_2$ with Chalcopyrite-Type Structure

YOSUKE FUJII[1,2,3] and ATSUKO KOSUGA[2,4]

1.—Department of Electronics, Mathematics and Physics, Graduate School of Engineering, Osaka Prefecture University, Sakai 599-8531, Japan. 2.—Department of Physical Science, Graduate School of Science, Osaka Prefecture University, Sakai 599-8531, Japan. 3.—e-mail: su104020@edu.osakafu-u.ac.jp. 4.—e-mail: a-kosuga@p.s.osakafu-u.ac.jp

Polycrystalline $CuGaTe_2$ with a chalcopyrite-type structure consolidated by hot-pressing is a potential candidate as a medium-temperature thermoelectric (TE) material. However, its high-temperature formation phases have rarely been reported to date. Here, we investigated the temperature-dependent formation phases and crystal structure at 300–800 K of hot-pressed $CuGaTe_2$. From synchrotron x-ray diffraction data and crystal structure analysis of the heating and cooling processes, it was clarified that a certain amount of impurity phases, such as Te and CuTe, precipitated from the $CuGaTe_2$ matrix when the temperature was increased (to 500–650 K). This is the temperature range where $CuGaTe_2$ has been reported to show high TE performance. After $CuGaTe_2$ was heated to 800 K, such impurity phases remained, even when cooled to room temperature. They also affected the tetragonal distortion and the x-coordinate of Te in the $CuGaTe_2$ matrix, probably due to deficiencies of Cu and Te in the matrix. Our results reveal detailed information on the formation phases of $CuGaTe_2$ at high temperature and thus provide insight for evaluation of its high-temperature stability and transport properties.

Key words: Thermoelectric, chalcopyrite-type structure, crystal structure analysis, hot-press, $CuGaTe_2$, synchrotron x-ray diffraction

INTRODUCTION

Chalcopyrite-type structure materials have previously been developed for various applications in photovoltaic and optoelectronics fields because of their characteristics can be controlled through selection of their atomic composition. The ternary chalcopyrite-type structure, denoted as $A^{I}B^{III}X_2^{VI}$ (A = Cu or Ag; B = Al, Ga or In; and X = S, Se or Te), can feature many different combinations of compositions. This structure is regarded as the stacking of two binary II–VI zinc-blended structures along the c-axis, in which one cation of a group II element is alternately replaced by two different cations of group I and III elements. This replacement alters the crystal structure from a cubic to a tetragonal shape and induces characteristic p–d hybridization between cations and anions. The degrees of tetragonality and hybridization differ according to the kinds of elements and temperature. These factors have a considerable effect on the physical properties of chalcopyrite-type structured materials. For example, typical chalcopyrite-type structure materials have good electrical properties and high thermal conductivity for thermoelectric (TE) applications. These properties are attributed to both the covalent and iconic bonding in the crystal structure, where two different cation atoms (I and III) are located at the inequivalent sites.[1] Therefore,

(Received August 8, 2017; accepted November 6, 2017; published online November 21, 2017)

improving the TE properties of chalcopyrite-type structured materials has been widely examined from the viewpoint of tuning their crystal structure. For example, this is done through the application of band structure engineering to form a pseudo-cubic structure[2] and reducing thermal conductivity by increased lattice distortion[3] and improving the figure of merit zT with anion displacement.[4] However, the temperature dependence of modifications of chalcopyrite-type crystal structures has not been extensively studied. For example, $CuGaTe_2$ is recognized as a prominent chalcopyrite-type structure TE material because of its high zT value at intermediate temperatures 700–900 K. There have been some reports of the phase diagram of pseudo-binary Cu_2Te-Ga_2Te_3,[5] the phase diagram of a ternary Cu-Ga-Te system at 923 K,[6] and the occurrence of order–disorder transition over 1000 K.[7] However, the thermal stability of $CuGaTe_2$ over its operating temperature range has not been previously reported in detail. Many attempts have been made to improve the TE properties of hot-pressed $CuGaTe_2$; however, these have been founded on the assumption that the material is stable over the operating temperature range, which has not been confirmed. For practical applications, TE materials should have long-operating lifetimes and be maintenance-free. Therefore, it is essential to consider the thermal stability of such materials to assess their reliability. Such studies also offer prospects for improving TE properties and understanding the material behavior at high temperatures. At elevated temperatures, mechanisms of material deterioration, such as oxidation, dissociation, and precipitation of constituent elements, can easily alter or lower TE performance. For example, tellurium is a typical element likely to dissociate from compounds below its melting temperature.[8–10] For these reasons, it is necessary to clarify the high-temperature phase formation of TE materials.

In the research presented herein, we focus on the chalcopyrite-type structure $CuGaTe_2$, prepared by hot-pressing, and examine its thermal stability, with the intention of understanding its potential applications to waste heat recovery at high temperatures. Because hot-pressing is a typical sintering method, it is also expected to be effective for $CuGaTe_2$. A previous report on hot-pressed $CuGaTe_2$ showed $zT = 1.4$ at 950 K.[11] Therefore, we investigated the thermal stability of hot-pressed $CuGaTe_2$ over an appropriate operating temperature range by observing phase changes and by performing crystal structure analysis. Hence, we studied phases of a $CuGaTe_2$ material that have already been evaluated for their TE properties, with the aim of providing information about the thermal stability of $CuGaTe_2$. We performed Rietveld analysis using fine profile data obtained by synchrotron x-ray powder diffraction and succeeding in capturing the phase formed in hot-pressed $CuGaTe_2$ at a high temperature.

EXPERIMENTAL SECTION

Sample Preparation

The starting materials, Cu (99.99% purity, shot, Rare Metallic Co., Ltd., Japan), Ga_2Te_3 (99.999% purity, chunks, Furuuchi Chemical Co., Ltd., Japan), and Te (99.999% purity, shot, Rare Metallic Co., Ltd., Japan), were mixed according to the corresponding stoichiometry and placed in a vacuumed silica tube. The mixture was melted at 1173 K and kept overnight in a furnace before being quenched in water. The obtained $CuGaTe_2$ ingot was annealed at 773 K for 72 h to obtain a homogeneous bulk sample. The samples had a dark gray appearance and no changes in the apparent color of the sample occurred on standing under atmosphere for several months. The ingot was then crushed into fine powder. The fine powder sample was sintered into a disc-like shape with a hot-press apparatus by applying conditions reported previously.[11] The hot-pressed sample was crushed into fine powder and was sealed into a 0.1 mm ϕ silica capillary under vacuum for synchrotron x-ray diffraction (SXRD) measurements.

To characterize the crystal structure and identify impurity phases, SXRD was performed at the BL02B2 beamline of the synchrotron radiation facility SPring-8. At beamline BL02B2, a large Debye–Scherrer camera and imaging plate (IP) were used for the detector. The wavelength used in this study was 0.419712 Å refined with CeO_2. We measured diffraction profiles of hot-pressed $CuGaTe_2$ with increasing temperature from 300 K to 800 K (in increments of 50 K), and then with decreasing temperature from 800 K to 300 K, for the purpose of observing changes in crystal structure and/or the development of impurity phases with changes in temperature.

Crystal Structure Refinement

Rietveld analyses were carried out for the observed SXRD profiles using the RIETAN-FP program[12] to refine the lattice parameters and to identify the appearance of phases. A modified split pseudo-Voigt function with Lorentz and Gauss functions full width at half maximum (FWHM) were applied for profile function. Impurity profiles were identified using data analysis software integrated with the x-ray powder diffraction software (PDXL; Rigaku Corporation).

RESULTS AND DISCUSSION

The SXRD patterns of hot-pressed $CuGaTe_2$ were collected using the heating process over 300–800 K in increments of 50 K (Fig. 1a and b), and then using the cooling process over 800–300 K in increments of 100 K (Fig. 1c and d). We analyzed the overall changes in SXRD patterns resulting from the variation in temperature. We found that the chalcopyrite-type structure was the main phase at

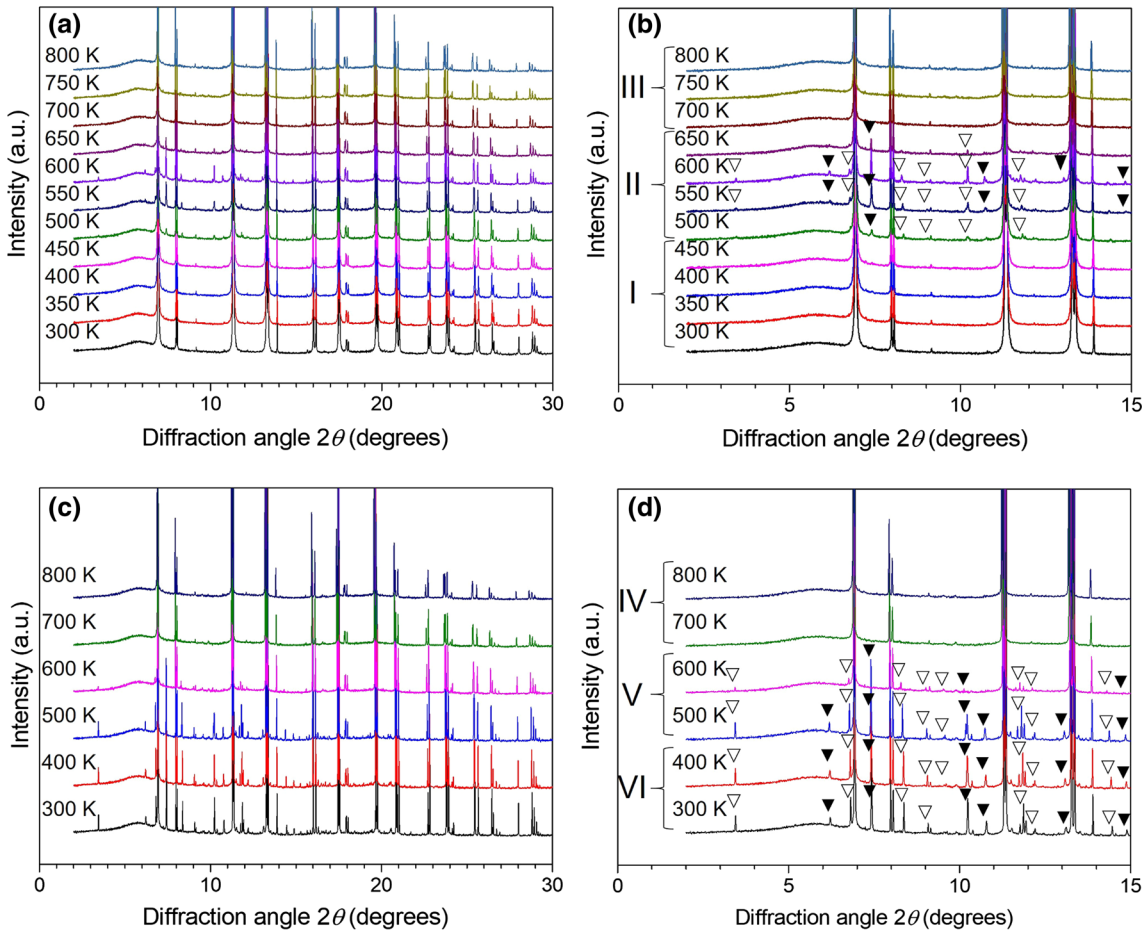

Fig. 1. Synchrotron x-ray diffraction (SXRD) measurements. (a) SXRD data of heating process over the temperature range 300–800 K. (b) Enlarged profile data of (a) at the angle range of 0°–15°. (c) SXRD data of cooling process over the temperature range 800–300 K. (d) Enlarged profile data of (c) at the angle range of 0°–15°. Triangles in (b and d) show locations of impurity peaks, with filled triangle denoting Te and open triangle denoting CuTe. Triangles are placed only where peaks can be glanced. The numbers I–VI refer to temperature regions to classify the profiles, herein referred to as region I, region II, etc.

all temperatures studied. During the heating process there existed only peaks of the chalcopyrite-type structure over the range 300–450 K (region I); the peaks of impurity phases appeared over the range 500–650 K, as denoted by triangle symbols (region II); then, the impurity phases disappeared, and only the chalcopyrite phase existed over the range 700–800 K (region III). During the temperature cooling process of 800–500 K (regions IV and V), the formation phases are the same as those observed during the heating process (regions III and II). The impurity phases, observed over the range 650–500 K, did not disappear below 500 K (region VI) and still remained at 300 K, which is different behavior from that observed during the heating process.

To observe the changes with temperature in the formation of phases and crystal structure of the hot-pressed $CuGaTe_2$, we identified the impurity phases using PDXL software and performed Rietveld analysis. The results of the Rietveld refinement are listed in Table I. At 300 K of region I, all of the peaks were fully indexed as those of $CuGaTe_2$ with a chalcopyrite-type structure, confirming previously reported data for samples prepared by similar methods.[11] The R-factors R_B and R_{wp} of this analysis were suppressed to $< 6\%$, meaning that good convergence was obtained. Likewise, in regions I and III, all of the peaks were fitted well to those of a chalcopyrite-type structure. In regions II, V, and VI, the peaks of the impurity phases correspond to those of Te and CuTe. Based on this finding, we carried out Rietveld analysis, assuming that the SXRD pattern contained $CuGaTe_2$ with chalcopyrite-type structure as the main phase, and Te and CuTe phases as the impurity phases. The resulting R-factors (R_{wp} and R_B) became $< 6\%$ and reached good convergence. In region II, the estimated phase fractions of Te and CuTe in the heating process were *ca*. 1 wt.% at 500 K, and reached maximum values of 2.41 wt.% and 1.69 wt.%, respectively, at 600 K, before starting to decrease when the temperature reached 650 K. Finally, it became zero at and above 700 K in region III. The melting temperature of Te

Table I. Parameters from SXRD data with Rietveld analysis for all temperatures of the heating (300–800 K) and cooling (700–300 K) processes

	Temperature (K)		300	350	400	450
$CuGaTe_2$	Cu $(4a)^a$	U (Å^2)	0.015 (11)	0.020 (13)	0.022 (14)	0.027 (2)
	Ga $(4b)^a$	U (Å^2)	0.015 (10)	0.015 (10)	0.017 (12)	0.018 (12)
	Te $(8d)^a$	x	0.2427 (2)	0.2430 (2)	0.2434 (3)	0.2435 (3)
		U (Å^2)	0.0102 (14)	0.0118 (14)	0.0135 (2)	0.0153 (2)
	a (Å)		6.0240 (10)	6.0272 (10)	6.0301 (10)	6.0339 (10)
	c (Å)		11.9368 (2)	11.9411 (2)	11.9447 (2)	11.9502 (2)
	η		0.991	0.991	0.990	0.990
	V (Å^3)		433.17 (10)	433.79 (10)	434.33 (10)	435.08 (11)
	R_B (%)		1.84	1.71	2.28	1.58
Phase fraction (wt.%)	$CuGaTe_2$		100	100	100	100
	Te		–	–	–	–
	CuTe		–	–	–	–
	GOF		1.41	1.34	1.31	1.33
	R_{wp} (%)		5.75	5.50	5.39	5.48

	Temperature (K)		500	550	600	650
$CuGaTe_2$	Cu $(4a)^a$	U (Å^2)	0.028 (2)	0.035 (2)	0.036 (2)	0.038 (2)
	Ga $(4b)^a$	U (Å^2)	0.022 (12)	0.020 (2)	0.023 (2)	0.025 (13)
	Te $(8d)^a$	x	0.2436 (3)	0.2448 (5)	0.2448 (4)	0.2445 (4)
		U (Å^2)	0.0166 (12)	0.018 (2)	0.0196 (2)	0.0216 (2)
	a (Å)		6.0378 (10)	6.0422 (10)	6.04506 (6)	6.04911 (6)
	c (Å)		11.9558 (2)	11.9625 (14)	11.9653 (13)	11.9699 (11)
	η		0.99	0.99	0.99	0.989
	V (Å^3)		435.84 (10)	436.73 (10)	437.24 (10)	438.00 (10)
	R_B (%)		1.02	1.87	2.43	2.18
Phase fraction (wt.%)	$CuGaTe_2$		98.29	96.65	95.9	99.41
	Te		0.62	1.99	2.41	0.59
	CuTe		1.08	1.36	1.69	–
	GOF		1.16	1.22	1.17	1.07
	R_{wp} (%)		4.81	5.04	4.80	4.44

Table I. continued

	Temperature (K)		700	750	800	700
$CuGaTe_2$	Cu (4*a*)[a]	*U* (Å^2)	0.047 (2)	0.053 (2)	0.065 (2)	0.049 (2)
	Ga (4*b*)[a]	*U* (Å^2)	0.026 (14)	0.029 (14)	0.029 (10)	0.027 (2)
	Te (8*d*)[a]	*x*	0.2451 (5)	0.2451 (5)	0.2464 (4)	0.2452 (5)
		U (Å^2)	0.0240 (2)	0.0265 (2)	0.0286 (2)	0.0249 (2)
	a (Å)		6.05409 (6)	6.05910 (6)	6.06242 (6)	6.0544 (10)
	c (Å)		11.9753 (12)	11.9811 (12)	11.9837 (12)	11.9764 (12)
	η		0.989	0.989	0.988	0.989
	V (Å^3)		438.92 (10)	439.86 (10)	440.44 (10)	439.00 (10)
	R_B (%)		2.24	2.71	2.41	2.79
Phase fraction (wt.%)	$CuGaTe_2$		100	100	100	100
	Te		–	–	–	–
	CuTe		–	–	–	–
	GOF		1.08	1.09	1.10	1.18
	R_{wp} (%)		4.48	4.63	4.66	5.04

	Temperature (K)		600	500	400	300
$CuGaTe_2$	Cu (4*a*)[a]	*U* (Å^2)	0.036 (2)	0.030 (2)	0.023 (12)	0.0166 (10)
	Ga (4*b*)[a]	*U* (Å^2)	0.024 (11)	0.018 (10)	0.014 (10)	0.0115 (8)
	Te (8*d*)[a]	*x*	0.2439 (3)	0.2443 (3)	0.2438 (3)	0.2433 (2)
		U (Å^2)	0.0198 (2)	0.0160 (2)	0.0126 (13)	0.0095 (12)
	c (Å)		11.9651 (10)	11.9567 (10)	11.9595 (10)	11.9410 (10)
	η		0.99	0.99	0.991	0.991
	V (Å^3)		437.13 (10)	435.77 (10)	434.63 (10)	433.42 (10)
	R_B (%)		2.31	2.15	1.63	2.23
Phase fraction (wt.%)	$CuGaTe_2$		98.85	91.49	91.25	91.48
	Te		0.05	4.07	4.35	4.26
	CuTe		1.10	4.44	4.41	4.26
	GOF		1.11	1.25	1.25	1.31
	R_{wp} (%)		4.64	5.21	5.23	5.47

Values are as follows: goodness of fit (GOF) and *R*-factors R_B and R_{wp}. Lattice constants *a* and *c*; tetragonal distortion, η; and lattice volume, *V*, of chalcopyrite-type structure. *U*: isotropic temperature factor of Cu, Ga, and Te. *x*: *x*-coordinate of Te. Occupancy of all sites was fixed to 100%.[a]Atomic positions: Cu 4*a* (0, 0, 0); Ga 4*b* (0, 0, 1/2); and Te 8*d* (*x*, 1/4, 1/8).

and CuTe was higher than 650 K, these impurities phases was not considered to melt. Instead, the eutectic reaction between Te and CuTe occurs at 613 K, so that Te and CuTe would change to liquid phase.[13] Thereby, the peaks of Te and CuTe were disappeared in region III, and the same phenomena can be occurred in region IV. In the cooling process of regions V and VI, Te and CuTe had values for the phase fraction of greater than 4 wt.% and retained a similar value even at 300 K. This implies that once the hot-pressed $CuGaTe_2$ was heated to 800 K, the Te and CuTe phases segregated from the $CuGaTe_2$, probably causing Cu and Te deficiencies in the $CuGaTe_2$-matrix phase at 300 K.

Figure 2a, b, and c show the temperature dependent tetragonal lattice parameters, a and c; the tetragonal distortion, defined by $\eta = c/2a$; and the x-coordinate of Te, respectively. The latter two parameters of η and x are features of a chalcopyrite-type structure. The ternary I–III–VI_2 chalcopyrite-type structure is regarded as the stacking of two binary II–VI zinc-blended structures along the c-axis, as mentioned. For example, ZnTe with a zinc-blend structure (Fig. 3a) is the binary analog of $CuGaTe_2$ with a chalcopyrite-type structure (Fig. 3b) drew using the software of visualization for electronic structural analysis (VESTA).[14] This type of crystal structure often shows tetragonal distortion, where η deviates from 1. In the ZnTe structure, each Te atom is tetrahedrally coordinated

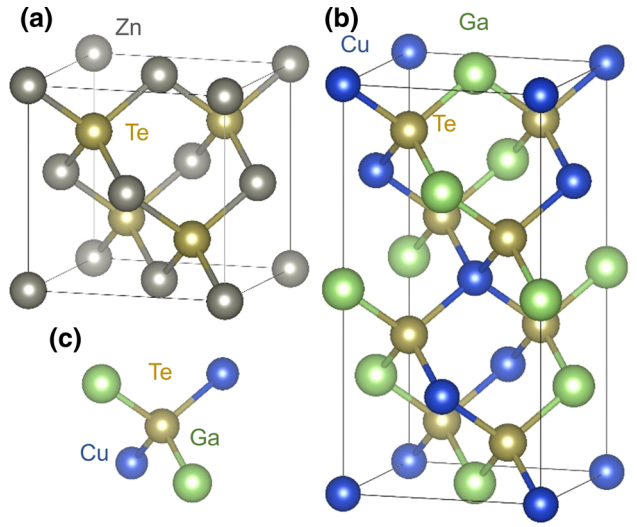

Fig. 3. (a) Crystal structure of ZnTe with zinc-blende structure, (b) $CuGaTe_2$ with chalcopyrite-type structure, and (c) tetrahedral structure of Cu_2Ga_2-Te in chalcopyrite-type structure.

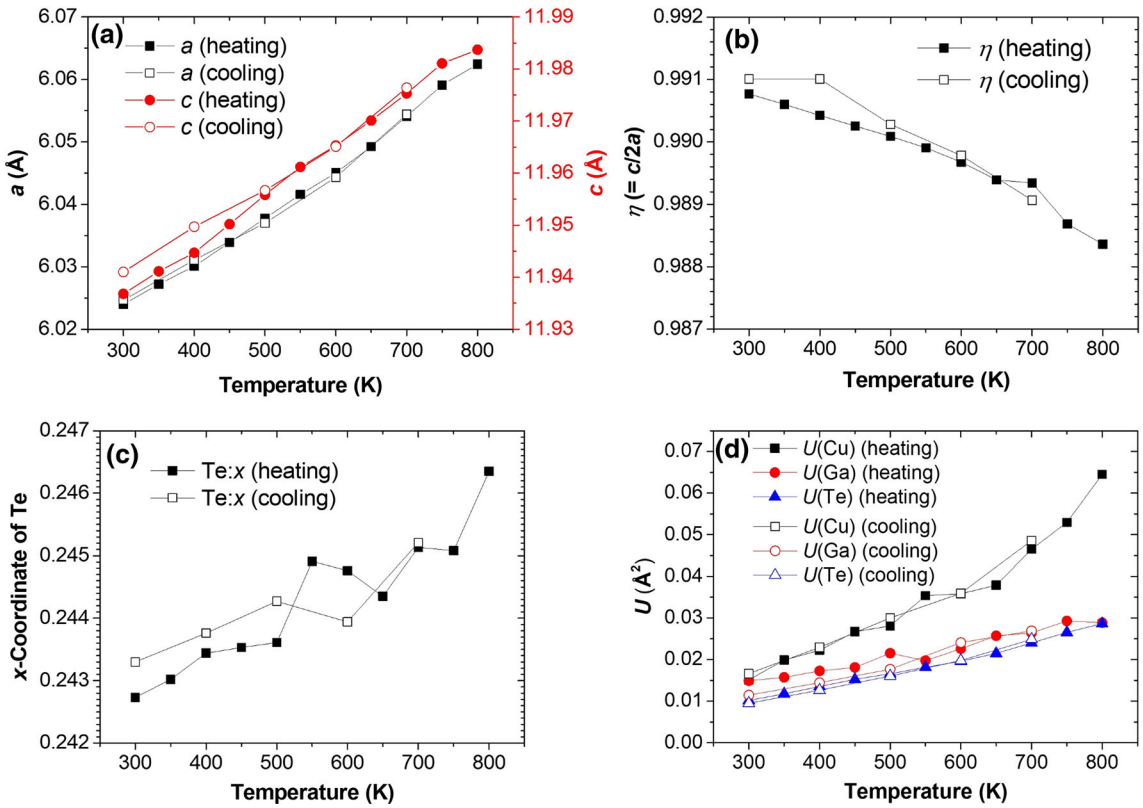

Fig. 2. Parameters obtained by Rietveld analysis. The parameters are shown for both heating and cooling processes, filled and white symbols show the heating and cooling process, respectively. (a) Temperature dependence of lattice constants a and c. (b) Temperature dependence of tetragonal distortion, η. (c) Temperature dependence of x-coordinate of Te. (d) Temperature dependence of isotropic temperature factor of Cu, Ga, and Te.

by four Zn atoms, meaning that the Te atom is located at the center of a tetrahedron. However, in the $CuGaTe_2$ structure each Te is coordinated by two Cu and two Ga atoms (Fig. 3c). This fact causes the Te to commonly adopt an equilibrium position closer to one pair of cations than to the other, i.e., Te atoms are displaced from their zinc-blende sites. This also mean that bonding states inside the Te-centered tetrahedron affect the η and x values in chalcopyrite compounds. Therefore, if some defects, such as point defects and/or antisite defects, are introduced to $CuGaTe_2$, η and x in defect $CuGaTe_2$ are expected to deviate from those in non-defect $CuGaTe_2$. a and c increased with an increase in temperature because of thermal expansion of the lattice. The calculated thermal expansion coefficient of a for regions I, II, and III during the heating process are $10.8 \times 10^{-6}\ K^{-1}$, $12.6 \times 10^{-6}\ K^{-1}$, and $1.38 \times 10^{-6}\ K^{-1}$, respectively. Those of c are $7.33 \times 10^{-6}\ K^{-1}$, $7.86 \times 10^{-6}\ K^{-1}$, and $7.02 \times 10^{-6}\ K^{-1}$, respectively. The thermal expansion coefficient of a increased as heating proceeded. That of c also increased, but that behavior did not show a monotonic increase; for region III the value is smaller than for regions I and II. It is expected, therefore, that removal of Cu and Te would have a greater effect on c than a. On the other hand, during the cooling process, a and c decreased with a decrease in temperature to follow the same root as in the heating process from thermal shrinkage of the lattice. However, the values of c at 300 and 400 K during the cooling process (region VI) are somewhat greater than those during the heating process (region I). This was probably affected to some extent by removal of Cu and Te elements from the matrix $CuGaTe_2$ phase, resulting from precipitation of the impurity phases of CuTe and Te. Such occurrences of change in an atomic level structure with temperature would cause a temperature dependent variation in η and x. As shown in Fig. 2b, η decreased with an increase in temperature because the thermal expansion coefficient of a is larger than that of c. In comparison with the η value in the heating process in region I, the η value in the cooling process in region VI is closer to 1 at room temperature, reflecting the temperature dependent behavior of a and c in regions I and VI. As for Fig. 3c, broadly speaking, the x-coordinate of Te increased with an increase in temperature; however, in region II where the appearance and disappearance, respectively, of Te and CuTe occur, this tendency changed. This may be attributed to the change in bonding state inside the Te-centered tetrahedron. In particular, assuming that deficiency of Cu would occur, it is reasonable to suggest that Te is attracted to the Ga, resulting in a larger x, which is consistent with the obtained results that x in region VI is greater than that in region I. Figure 2d shows the temperature dependence of the isotropic temperature factor, U, of Cu, Ga, and Te. They increased with temperature, indicating enhanced thermal vibration of each atom. It is noted that the U of Cu is significantly larger than that of Ga and Te within the temperature range examined. This is not only because of the deficiency of Cu from the $CuGaTe_2$ matrix, but also because Cu atoms deviated significantly from their equilibrium positions. This is supported from molecular dynamics simulations reported previously.[15]

We clarified that by increasing the temperature Te and CuTe were separated from the $CuGaTe_2$ matrix in polycrystalline $CuGaTe_2$ samples consolidated by hot-pressing. At this stage it is not clear whether these phenomena would occur only in hot-pressed $CuGaTe_2$ so further study is needed to clarify this. However, our results do at least suggest that the high-temperature TE properties of hot-pressed $CuGaTe_2$ reported previously[11] could be affected by changes in phase formation that result from changes in temperature. Therefore, to evaluate the high-temperature transport properties and stability of $CuGaTe_2$ more precisely, it is necessary to analyze the experimental data under careful consideration of its temperature-dependent formation phases and crystal structure.

CONCLUSIONS

We investigated the thermal stability of hot-pressed thermoelectric $CuGaTe_2$ by measuring synchrotron x-ray diffraction data over the temperature range 300–800 K and performing crystal structure refinement. By carrying out crystal structure refinement we revealed that Te and CuTe can separate from the $CuGaTe_2$ matrix at the temperature range 550–650 K. By increasing the temperature to greater than 650 K, the Te and CuTe phases disappeared and are expected to have changed to liquid phase. The vacancy of Cu changes the fractional coordinates of Te and modifies the bonding state inside Te-centered tetrahedron. Furthermore, precipitation occurred after decreasing the temperature to < 500 K, meaning that the Te and CuTe phases are expected to remain after cooling. Isotopic temperature factor of Cu increased with temperature and is significantly larger than that of Ga and Te within the temperature range examined, which is likely to attribute to deficiency of Cu atoms and deviation from equilibrium position. Therefore, we should consider that the separated phases can affect the thermoelectric properties of such systems.

ACKNOWLEDGEMENTS

This work was supported by a Grant-in-Aid for Young Scientists (A) (No. 15H05548). Synchrotron radiation experiments were performed at SPring-8 with the approval of the Japan Synchrotron Radiation Research Institute (JASRI, Proposal Nos. 2014B1334, 2015A1363, and 2015B1377). We thank Prof. S. Yamanaka's group at Osaka University, Japan for conducting the hot pressing of $CuGaTe_2$.

REFERENCES

1. J.L. Shay, J.H. Wernick, and B.R. Pamplin, *Ternary Chalcopyrite Semiconductors: Growth, Electronic Properties, and Applications, Vol. 7 in International Series in the Science of the Solid State* (Amsterdam: Elsevier, 1975), pp. 110–128.
2. J. Zhang, R. Liu, N. Cheng, Y. Zhang, J. Yang, C. Uher, X. Shi, L. Chen, and W. Zhang, *Adv. Mater.* 26, 3848 (2014).
3. J. Yang, S. Chen, Z. Du, X. Liu, and J. Cui, *Dalton Trans.* 43, 15228 (2014).
4. Y. Lu, S. Chen, W. Wu, Z. Du, Y. Chao, and J. Cui, *Sci. Rep.* 7, 40224 (2017).
5. A. Congiu, L. Garbato, and P. Manca, *Mater. Res. Bull.* 8, 293 (1973).
6. H.-J. Wu and Z.-J. Dong, *Acta Mater.* 118, 331 (2016).
7. A. Zunger, *Appl. Phys. Lett.* 50, 164 (1987).
8. I.J. Ohsugi, D. Tokunaga, M. Kato, S. Yoneda, and Y. Isoda, *Mater. Res. Innov.* 19, 301 (2015).
9. S. Yoneda, M. Kato, and I.J. Ohsugi, *J. Theor. Appl. Phys.* 7, 11 (2013).
10. S. Yoneda, M. Kato, and I.J. Ohsugi, *J. Appl. Phys.* 107, 074901 (2010).
11. T. Plirdpring, K. Kurosaki, A. Kosuga, T. Day, S. Firdosy, V. Ravi, G.J. Snyder, A. Harnwunggmoung, T. Sugahara, Y. Ohishi, H. Muta, and S. Yamanaka, *Adv. Mater.* 24, 3622 (2012).
12. F. Izumi and K. Momma, *Solid State Phenom.* 130, 15 (2007).
13. A.S. Pashinkin and V.A. Fedorov, *Inorg. Mater.* 39, 539 (2003).
14. K. Momma and F. Izumi, *J. Appl. Crystallogr.* 44, 1272 (2011).
15. J.M. Yang, Y.L. Yan, Y.X. Wang, and G. Yang, *RSC Adv.* 4, 28714 (2014).